TID-4500, UC-35
Nuclear Explosions—
Peaceful Application

Lawrence Radiation Laboratory
UNIVERSITY OF CALIFORNIA
LIVERMORE

UCRL-50480

MOTIONS OF EARTH FILL DAMS DURING THE GASBUGGY EVENT

Dean V. Power

August 1968

MOTIONS OF EARTH FILL DAMS DURING THE GASBUGGY EVENT

Abstract

Measurements of motions were made on and near the Navajo and the El Vado Dams during the Gasbuggy detonation. These dams were 38 and 43 km, respectively, from the center of the detonation. The response of these earth-filled dams to the seismic motions from the Gasbuggy Event were analyzed in both the time (velocity) and frequency (power spectral density) domains. Amplification of ground motions were found to be dependent upon frequency and location. Resultant peak particle velocity amplitudes on the crest were found to be 2.1 times the base motion on the Navajo Dam and 2.7 times the base motion on the El Vado Dam. Peak power spectral densities were found to range from 3 or 4 times base motion to as much as 40 times base motion at the dam's resonant frequencies. Correlations of power spectral densities for different stations resulted in a determination of the frequencies for the first few natural modes. Shear wave velocities of about 1100 ft/sec in the fill material were calculated using these frequencies and a simple mechanical model of the dams.

Introduction

The Gasbuggy Event consisted of a nominal 26-kt explosive detonated at a depth of about 4250 ft at a location some 55 mi east of Farmington, New Mexico. Firing occurred at 12:30 PM, Mountain Standard time, on December 10, 1967. This experiment is one of a continuing series (commonly known as the Plowshare Program) being conducted for the purpose of investigating possible peaceful applications of nuclear explosives. The specific purpose of Gasbuggy was to investigate the feasibility of using nuclear explosives to stimulate tight gas fields.

In any Plowshare application there are several common concerns. One of these concerns is the effect upon nearby structures of the seismic disturbance generated by any underground explosion. A very common structure, prevalent throughout the world, is the earth fill dam. The purpose of this study is to investigate the

response of two earth fill dams to the seismic motions generated by Gasbuggy. The information gained will (1) provide an initial basis for safety criteria, and (2) indicate necessary future work to improve these criteria.

The dams included in this study are the Navajo Dam and the El Vado Dam at 38 and 42 km, respectively, from the detonation center. Their locations are shown in Fig. 1. Physical details of the Navajo Dam and El Vado Dam are shown in Figs. 2 and 3, respectively. The Navajo Dam is by far the largest, being 402 ft in maximum height with a base width of 2566 ft and a crest length of 3648 ft.[1] The following are the dimensions of the El Vado Dam: 1450 ft in crest length, 600 ft in maximum base width, and 180 ft in maximum height.[2]

The construction of the Navajo Dam is "typical" of most large earth fill dams. The El Vado Dam has one unique feature:

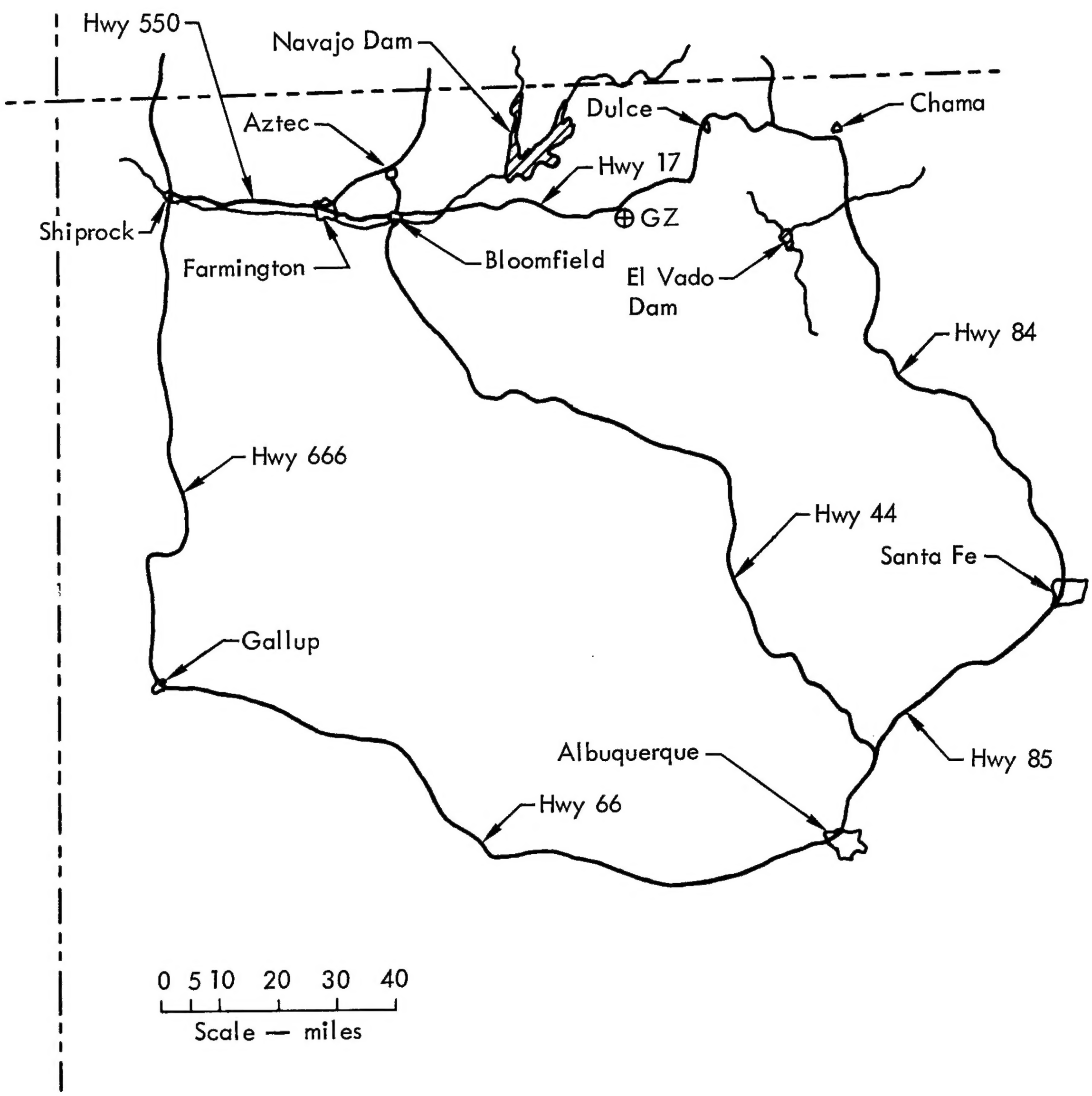

Fig. 1. Map of Northwest part of New Mexico showing locations of Gasbuggy Event and Navajo and El Vado Dams.

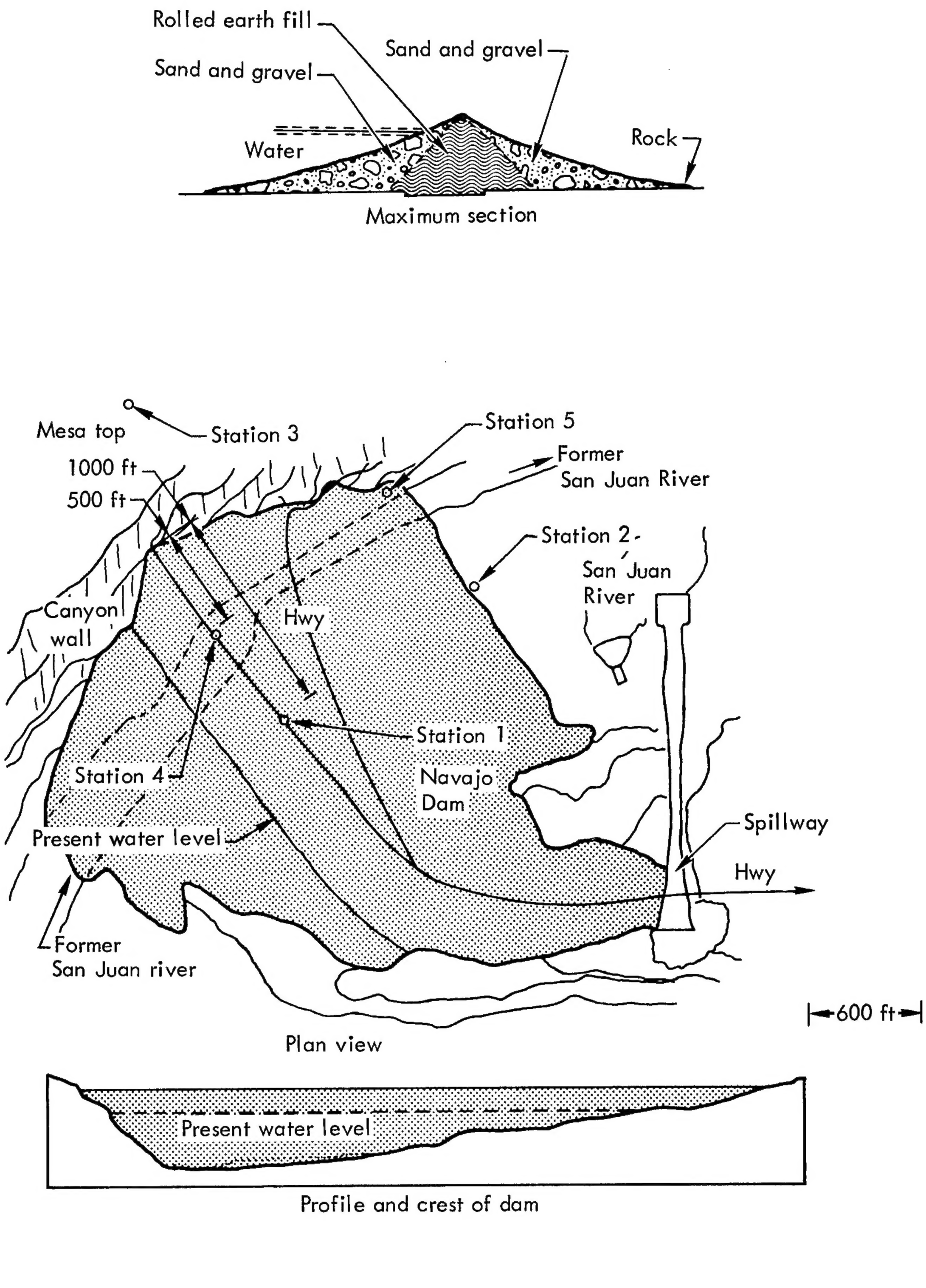

Fig. 2. Navajo Dam and associated seismic station locations.

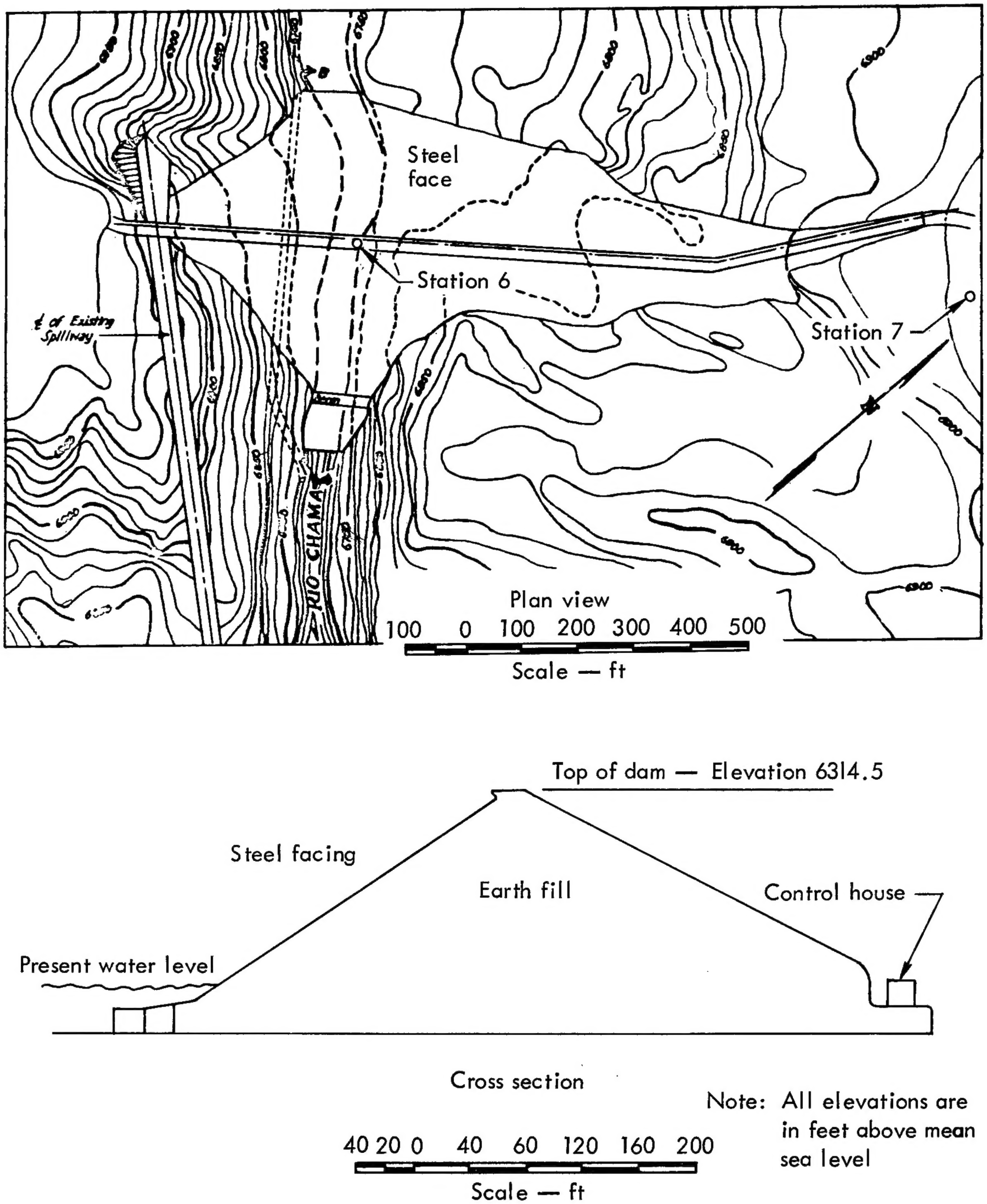

Fig. 3. El Vado Dam and associated seismic stations.

the water barrier consists of a welded, sheet-steel membrane covering the entire upstream face of the dam. This particular arrangement was apparently necessary due to the unstable nature of one of the abutments.

Procedure

The measurements in this study were made with moving coil velocity geophones of a type known as the HS10-1. This instrument has a 1.0-cps natural frequency, and sensitivity is determined by the coil impedance. Figure 4 shows the sensitivity curve for a typical instrument at 70% damping. Recording was made on four-track, portable, FM tape recorders which were designed at the Lawrence Radiation Laboratory.

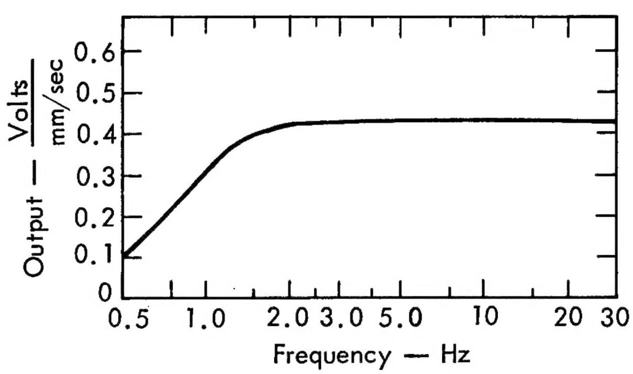

Fig. 4. Sensitivity curve for typical 1-cycle geophone used in this study (this curve is for 70% damping).

Each seismic station consisted of three orthogonally oriented instruments in a standard Cartesian array. The x component was always perpendicular to the long axis of the dam with which it was associated and in the horizontal plane. The other horizontal instrument, or y component, was parallel to the long axis of the dam. The z component was always vertical. All three instruments were mounted in a watertight canister and buried in a hole 4 ft in depth and 1 ft in diameter.

Seven stations were established, five on and near the Navajo Dam and two at El Vado Dam. These locations are shown in Figs. 2 and 3.

Following the event the taped records were digitized on an Astro-Data analog-to-digital translator. The digitized information was subsequently analyzed on IBM 7094 and CDC 3600 computers.

Analysis

The records obtained were analyzed in both the time domain and the frequency domain. The time history analysis provides information on velocity amplitudes, relative time of arrival and approximate frequency of various parts of the wave train. The last-named is arrived at by assuming sinusoidal motion and measuring the time between consecutive zero amplitudes. The computer code used is

called Vector. It can handle the three orthogonal signals from a given station simultaneously and calculates a time history for the resultant velocity vector.[3]

A more recent development in analysis capability is Power Spectral Density (PSD). This is a method of calculating the energy as a function of frequency in a wave train. A thorough discussion of this method is available in several texts.[3,4] The energy density is referred to as the PSD. Since the energy in each component of motion is independent of the other components, a resultant PSD is obtained by simple addition. A measure of the total energy in each component (referred to as E) is arrived at by integrating the PSD over all frequencies. A measure of the total station energy is the sum of the E's for the three components (referred to as ΣE). The total station energy may also be calculated by integrating the resultant PSD over all frequencies.

If several stations are to be compared it is important that the length of the record analyzed include, at least, all significant motion, and that all records be of the same length. This analysis used the first 40 sec of motion. In all cases the the amplitudes after 40 sec never exceeded 5% of the peak amplitude.

In comparing motions between stations, Stations 3 and 7 were treated as the base stations since they measured the motion at a location near the dams but far enough away to be unaffected by the proximity of the dam. It is assumed in the analysis that these motions were the driving motions for the dams, and the other stations recorded the response of the dams to that motion at the various locations. Correlations were made in both the time and frequency domains.

Results and Discussion

VELOCITY MEASUREMENTS

Table I shows the velocity information in tabular form. Shown are peak velocities, time of arrival of peak after first motion, and approximate frequency of peak motion for each component and the resultant at all stations. Also shown in Table I is the amplification factor (F_1) or the ratio of peak velocities between a given station and the base station.

Motions on the crest of Navajo Dam (Stations 1 and 4) were greater than the base station motions as one would expect for such a structure. However they did not significantly exceed the motions expected in an alluvial geology.[5*] The amplification was greater at the crest center than nearer the abutment in the x and z components; this condition was also expected. However the y motion is amplified more near the abutment than at the center. This might be expected because of the sloping interface between the dam and the canyon wall.

---

*See Fig. 39.

Table I. Time history domain (velocity) data.

Station	Component[a]	Peak velocity (cm/sec)	Time of arrival after first motion (sec)	Frequency of peak motion (Hz)	Amplification Factor, F_1
1	x	1.12	2.24	4.0	3.2
Center of crest	y	0.62	8.70	2.4	3.1
of Navajo Dam	z	1.41	4.40	2.4	2.1
	Res	1.50	4.40	—	2.1
2	x	0.59	2.81	4.5	1.7
Center of toe of	y	0.39	2.84	5.0	2.0
Navajo Dam	z	0.63	1.52	4.0	0.93
	Res	0.66	2.82	—	0.91
3	x	0.35	3.25	3.7	1.0
Base station	y	0.20	2.60	3.2	1.0
(top of mesa), Navajo Dam	z	0.68	1.63	3.7	1.0
	Res	0.73	1.63	—	1.0
4	x	0.91	3.0	4.5	2.6
Dam crest	y	1.02	2.80	2.5	5.1
(between center and abutment)	z	1.14	0.64	4.0	1.7
of Navajo Dam	Res	1.33	0.64	—	1.8
5	x	0.32	2.40	3.3	0.92
Downstream toe	y	0.23	1.87	4.0	1.1
(between center and abutment)	z	0.50	1.60	3.3	0.74
of Navajo Dam	Res	0.51	1.60	—	0.70
6	x	0.39	6.13	3.0	3.5
Center of crest	y	0.26	6.51	3.0	1.6
of El Vado Dam	z	0.20	2.75	4.0	1.7
	Res	0.43	6.13	—	2.7
7	x	0.11	8.16	2.0	1.0
Base station	y	0.16	4.76	4.0	1.0
(top of mesa), El Vado Dam	z	0.12	2.85	3.0	1.0
	Res	0.16	3.00	—	1.0

[a]x component = radial component; y component = transverse; z component = vertical; Res = resultant.

The motions at the toe of the Navajo Dam (Stations 2 and 5) showed considerably less amplification than those on the crest. This also was expected since there is only about 50 ft of fill under Stations 2 and 10, or 15 ft under Station 5. In fact, the amplification at Station 5 was for the most part, less than 1. At none of the

instrument locations on the Navajo Dam did the motion in any component exceed 2.1 times the maximum motion at Station 3, and no resultant exceeded 2.1 times the Station 3 resultant.

Similar results for the El Vado Dam are shown, the resultant for Station 6 being 2.7 times that for Station 7.

POWER SPECTRAL DENSITY MEASUREMENTS

The PSD's for all stations are shown in Figs. 5 through 11. Information extracted from these curves is given in Table II and includes the peak PSD in each component and resultant, the amplification factors over the base station for peak PSD (F_2), the frequency at which the peak occurred, the energy in each component (E), the total station energy (ΣE), and the amplification factors for E and ΣE (F_3).

Amplification of PSD is given as a function of frequency in Figs. 12 through 26 (Stations 3 and 7 are used as bases). The same correlation technique is used to compare stations on the Navajo Dam to other stations also on the dam. The crest stations are compared to the stations on the toe in Figs. 27 through 32, the crest stations are compared to each other in Figs. 33 through 35, and the stations at the toe are compared in Figs. 36 through 38. Since energy is proportional to the square of velocity, one would expect the amplification factors for the PSD to be the square of the amplification factors for velocity. A comparison of the values from Table I and Table II shows that this is indeed the general trend for both F_2 and F_3. For both velocity and PSD, Station 5 shows less motion than Station 3 and the largest amplification factor on the Navajo Dam occurs for the y component of Station 4.

This general trend is not present in every signal. A single-cycle, high-amplitude velocity pulse would not show up strongly in the PSD since this is an averaging process. From the standpoint of structures response, a single cycle is not as significant as a wave train of several or many cycles. Thus the PSD has its advantages over peak velocity when the effects of a signal upon a structure are considered.

Much more information about the dams may be gained by examining Figs. 12 through 38. Station 1, being at the approximate midpoint of the main body of the dam, is at the anti-node of the odd modes and the node of even modes of x motion. Station 4 is at the anti-node of the second mode. Figures 12 and 18 show the first strong amplification at about 1.4 Hz, indicating that this is the frequency of the first x mode. The amplification is down on Station 1 at 2 Hz but continues high at Station 4 indicating the second mode is at about 2 Hz. The latter point is shown more clearly on Fig. 36, where Stations 1 and 4 are compared directly. The third mode appears to be at about 2.5 Hz.

The first mode of y motion is at 1.7 Hz, and a second mode seems to be present at 2.5 Hz (Figs. 13 and 19). The first two z modes show up at 2.1 and 2.6 Hz, and a weaker third mode at 4.0 Hz (Figs. 14 and 20).

Figures 15 through 17 and 21 through 23 show near unity amplifications at the toe of the dam at the low frequency and small but significant amplifications only

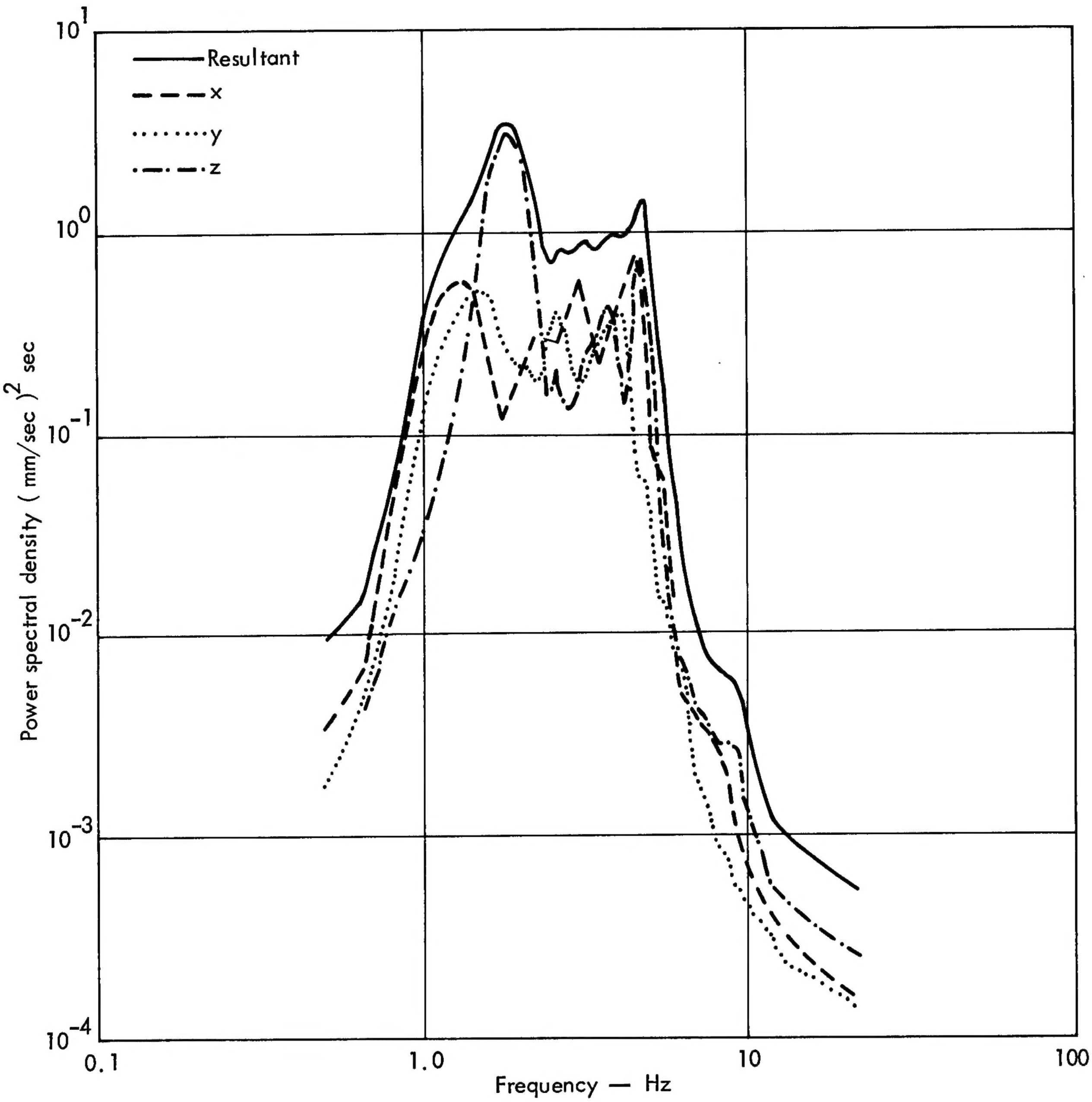

Fig. 5. Power spectral density for three components and resultant on Station 1 (center of crest of Navajo Dam).

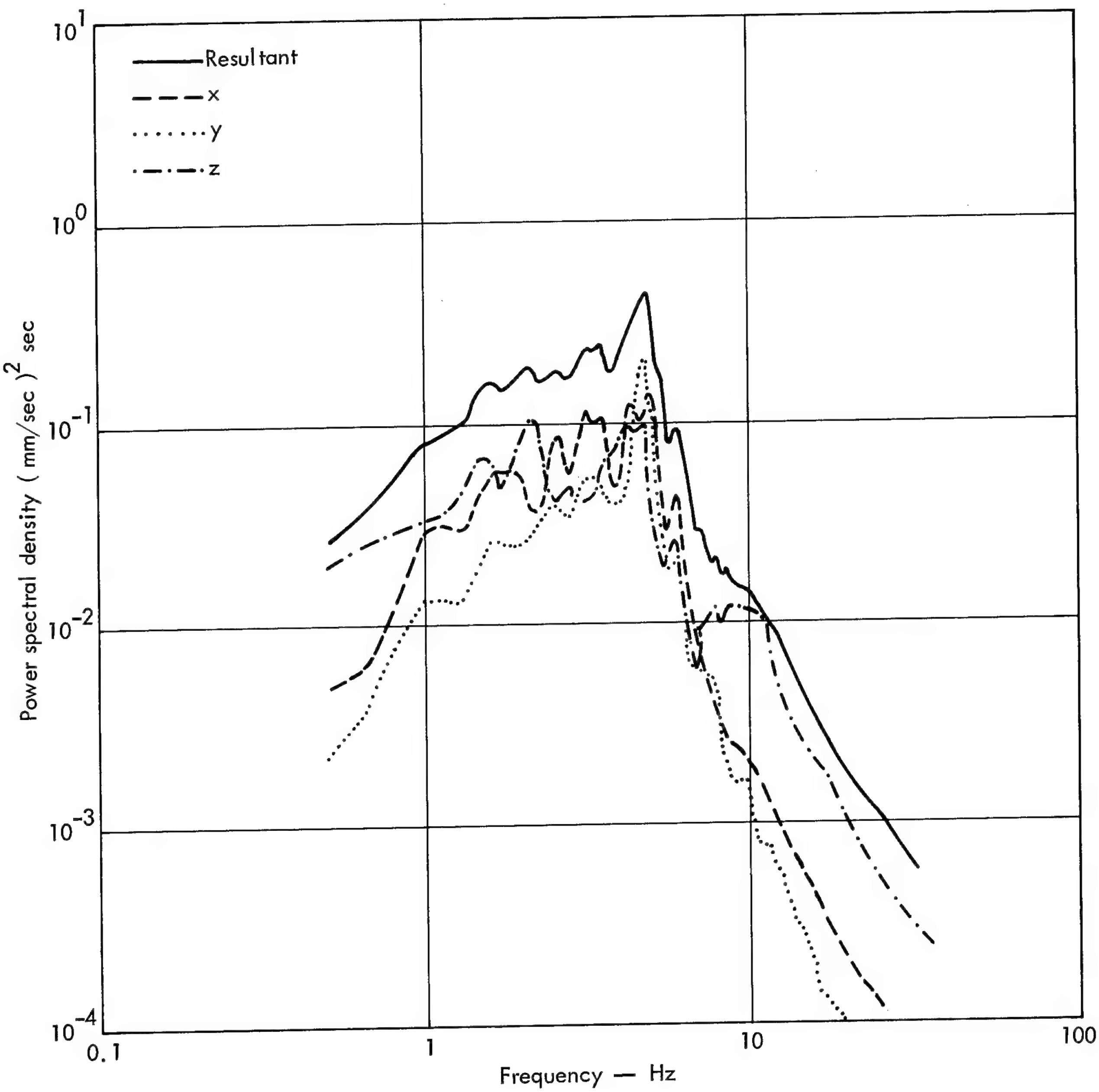

Fig. 6. Power spectral density for three components and resultant on Station 2 (center of downstream toe of Navajo Dam).

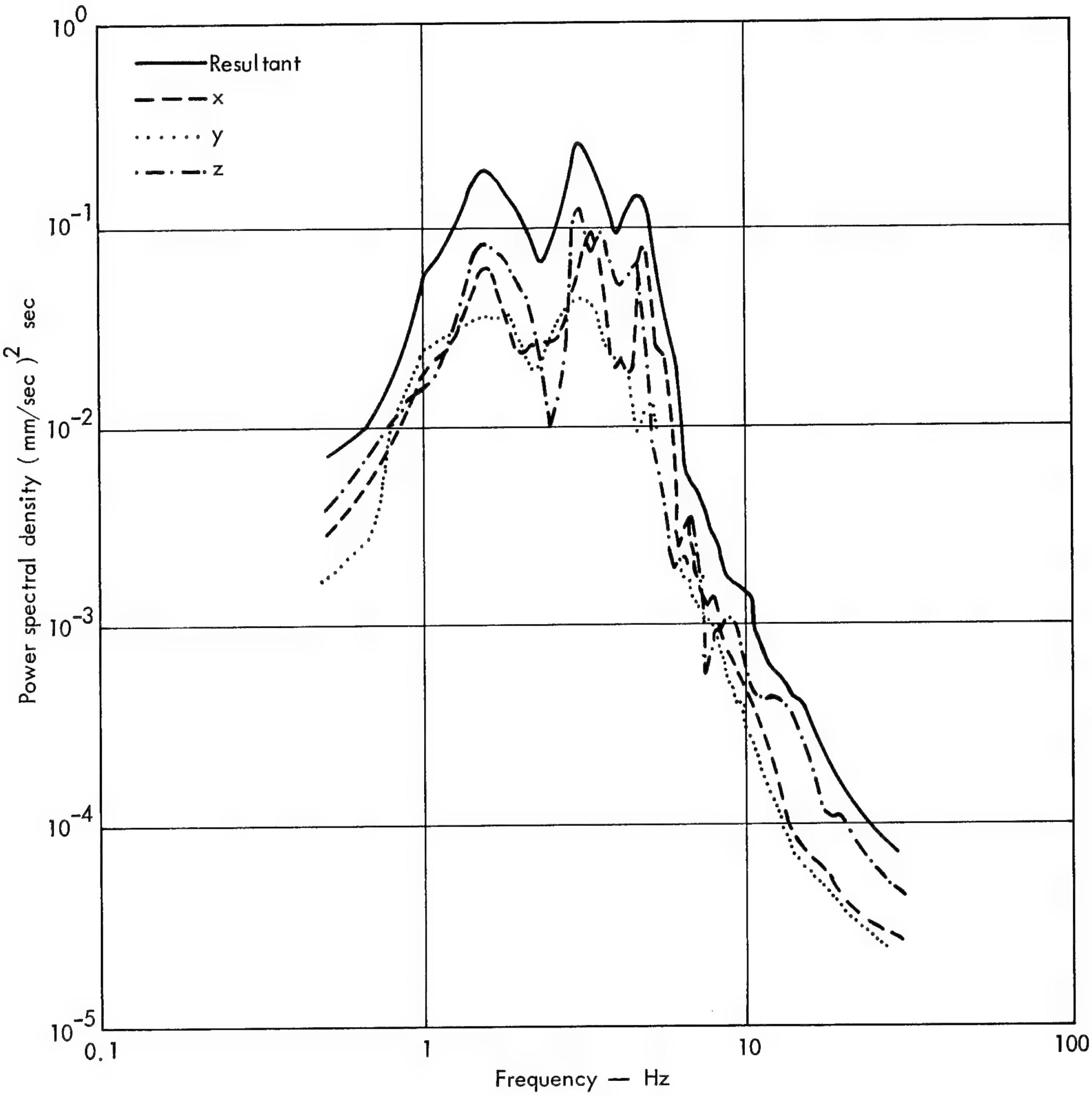

Fig. 7. Power spectral density for three components and resultant on Station 3 (base station, top of mesa, Navajo Dam).

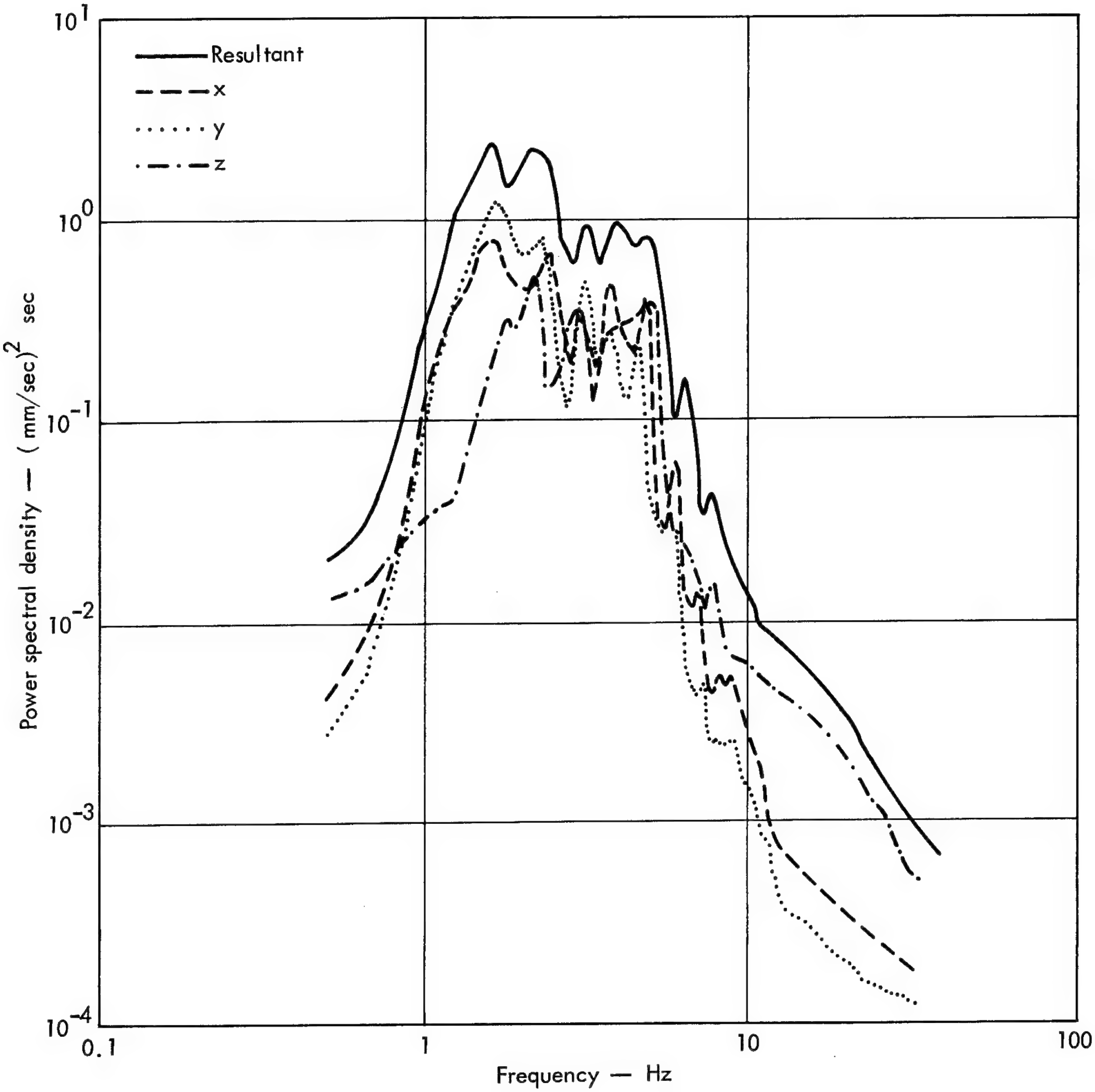

Fig. 8. Power spectral density for three components and resultant on Station 4 (dam crest—between center and abutment—of Navajo Dam).

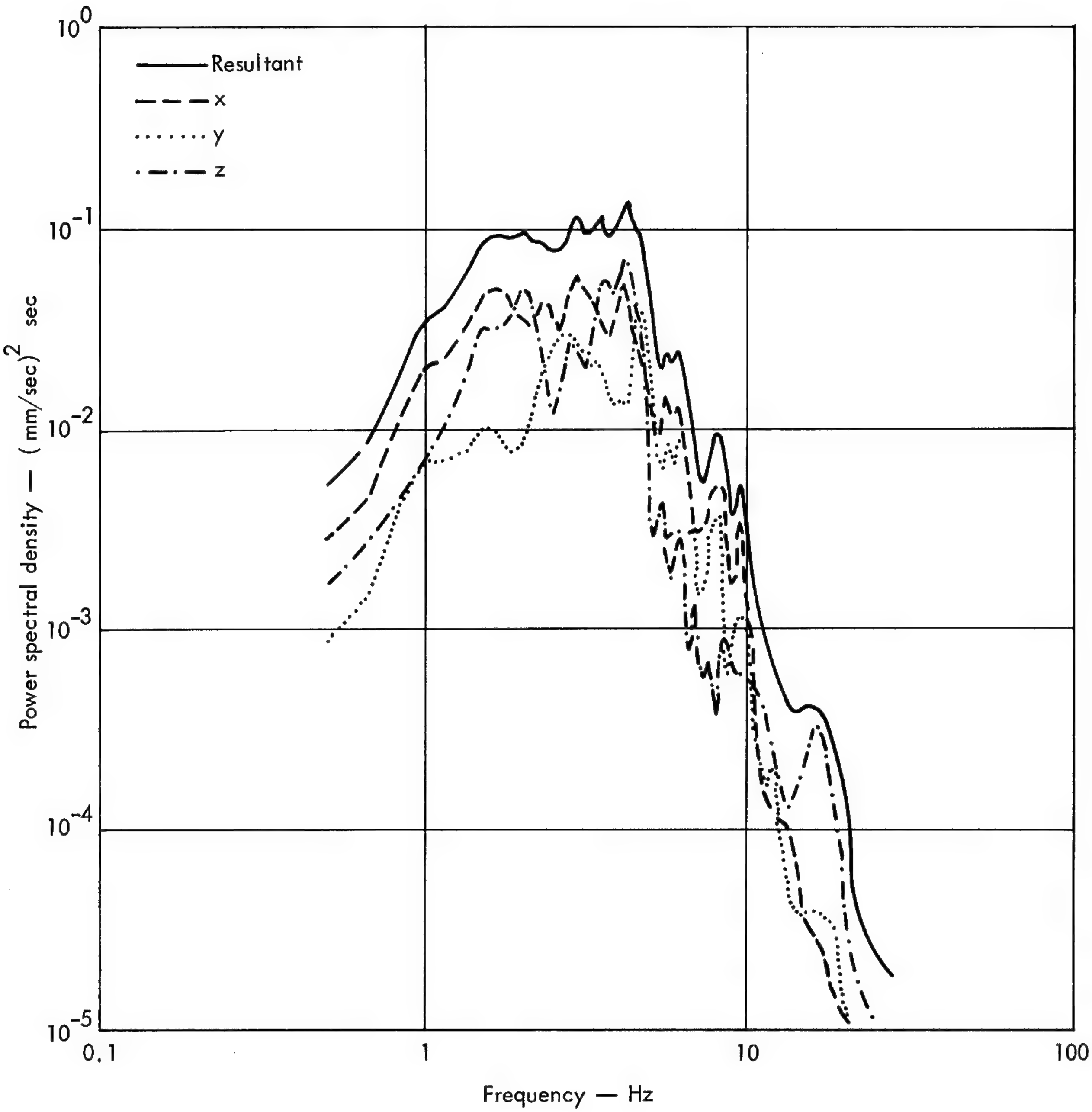

Fig. 9. Power spectral density for three components and resultant for Station 5 (downstream toe—between center and abutment—of Navajo Dam).

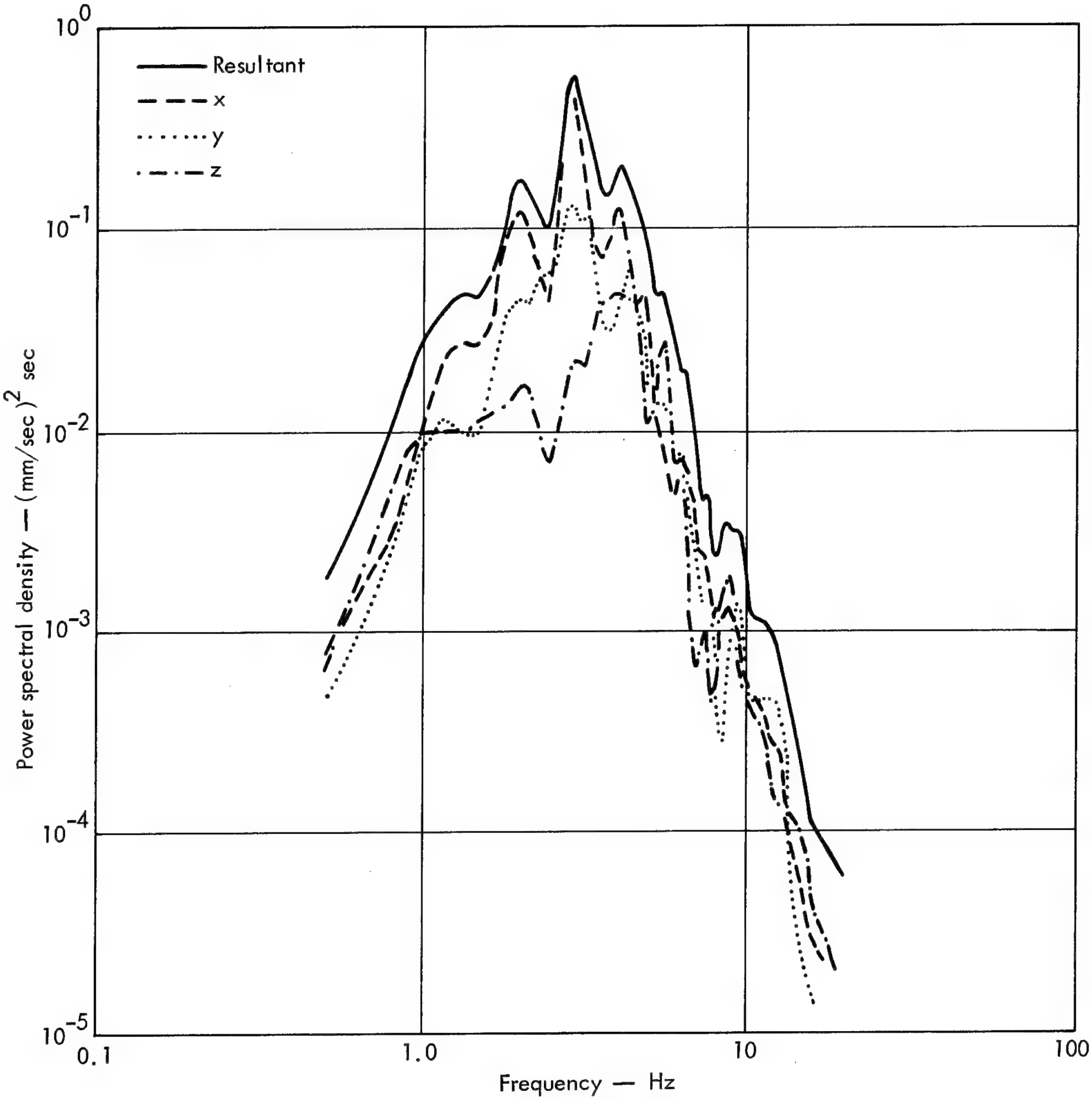

Fig. 10. Power spectral density for three components and resultant on Station 6 (center of crest of El Vado Dam).

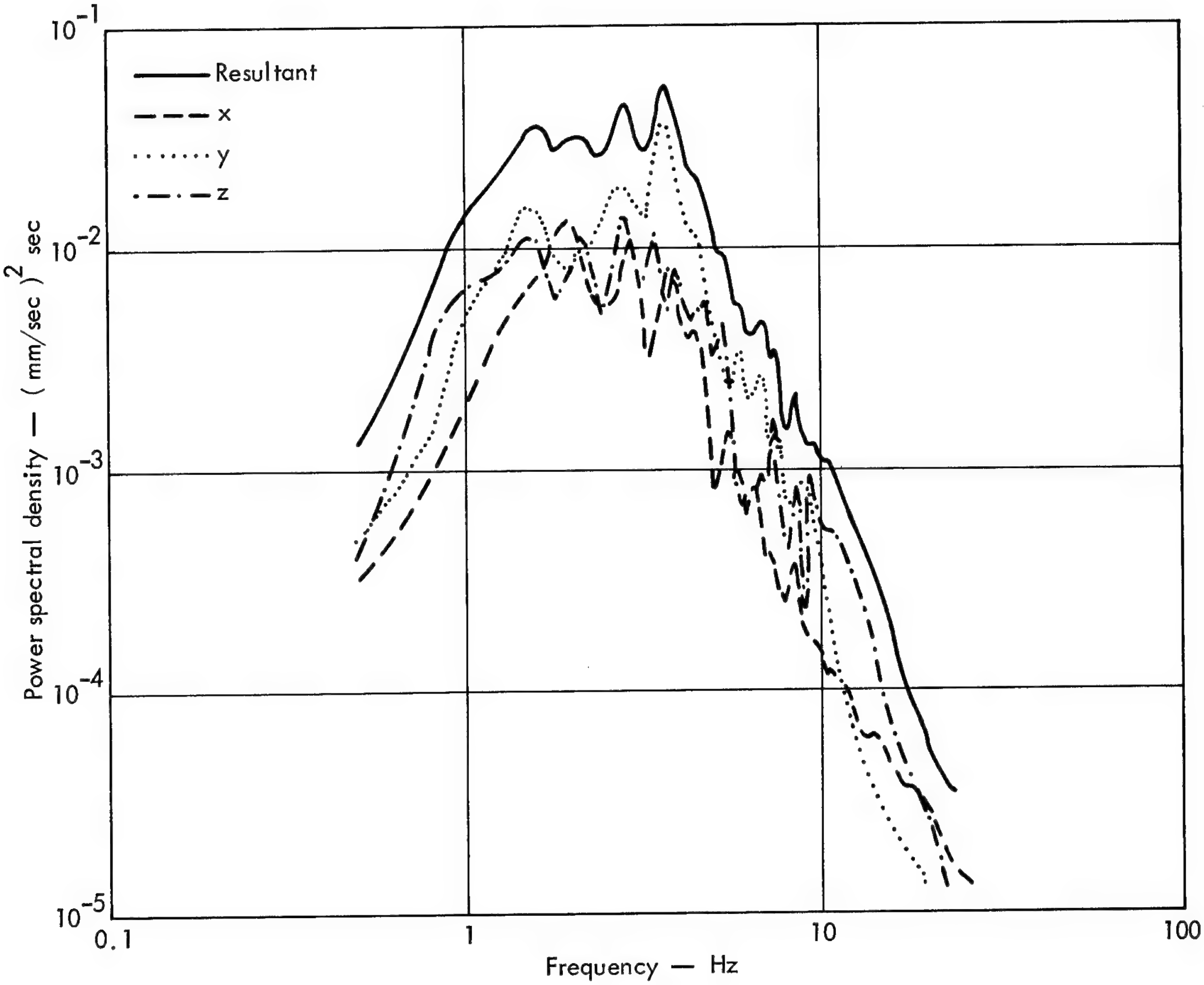

Fig. 11. Power spectral density for three components and resultant on Station 7 (base station, top of mesa, El Vado Dam).

Table II. Frequency domain (power spectral density) data.

Station	Component	Peak PSD $(mm/sec)^2 sec$	Amplification[a] factor, F_2	Frequency of peak PSD (Hz)	Total energy $(mm/sec)^2$ Component, E	Total energy $(mm/sec)^2$ Station, ΣE	Amplification factor, F_3
1	x	0.647	6.5	5.67	1.42		6.3
Center of crest	y	0.417	9.5	1.50	0.93		6.5
of Navajo Dam	z	2.64	20.1	1.83	2.39		11.9
	Res	2.95	11.8	1.83		4.73	8.3
2	x	0.148	1.5	5.0	0.475		2.1
Center of toe of	y	0.206	4.7	4.83	0.329		2.3
Navajo Dam	z	0.112	0.85	2.17	0.494		2.5
	Res	0.400	1.6	5.0		1.30	2.3
3	x	0.099	1.0	3.33	0.225		1.0
Base station	y	0.044	1.0	3.33	0.143		1.0
(top of mesa), Navajo Dam	z	0.131	1.0	3.17	0.201		1.0
	Res	0.251	1.0	3.17		0.569	1.0
4	x	0.864	8.7	1.67	1.80		8.0
Dam crest	y	1.31	29.8	1.67	1.85		13.0
(between center and abutment)	z	0.478	3.7	2.33	1.29		6.4
of Navajo Dam	Res	2.41	9.6	1.67		4.94	8.7
5	x	0.063	0.64	3.00	0.201		0.89
Downstream toe	y	0.044	1.0	4.67	0.104		0.73
(between center and abutment)	z	0.079	0.60	4.17	0.164		0.82
of Navajo Dam	Res	0.148	0.59	4.17		0.469	0.82
6	x	0.427	30.5	3.00	0.439		14.2
Center of crest	y	0.122	3.2	3.00	0.223		2.9
of El Vado Dam	z	0.045	3.2	4.00	0.120		2.7
	Res	0.560	10.8	3.00		0.783	5.2
7	x	0.014	1.0	2.00	0.031		1.0
Base station	y	0.038	1.0	3.67	0.077		1.0
(top of mesa) El Vado Dam	z	0.014	1.0	2.83	0.044		1.0
	Res	0.052	1.0	3.67		0.151	1.0

[a] F_2 is calculated from the peak regardless of the frequency at which it occurs. The frequency dependent amplification shown in Figs. 12 through 26 often exceeds values of F_2.

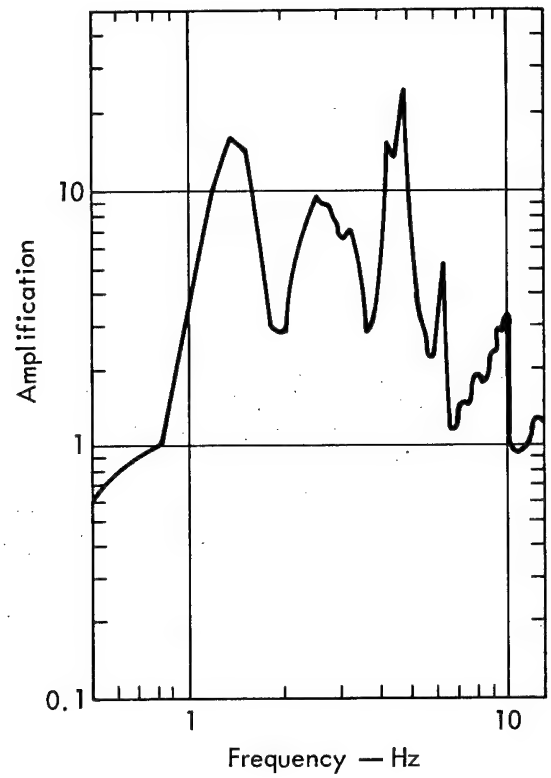

Fig. 12. Ratio of PSD's for Station 1 over Station 3 (x component)

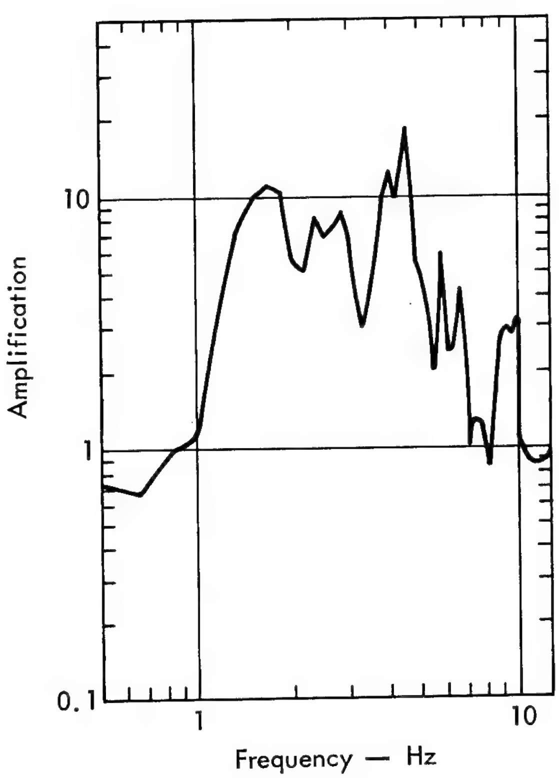

Fig. 13. Ratio of PSD's for Station 1 over Station 3 (y component).

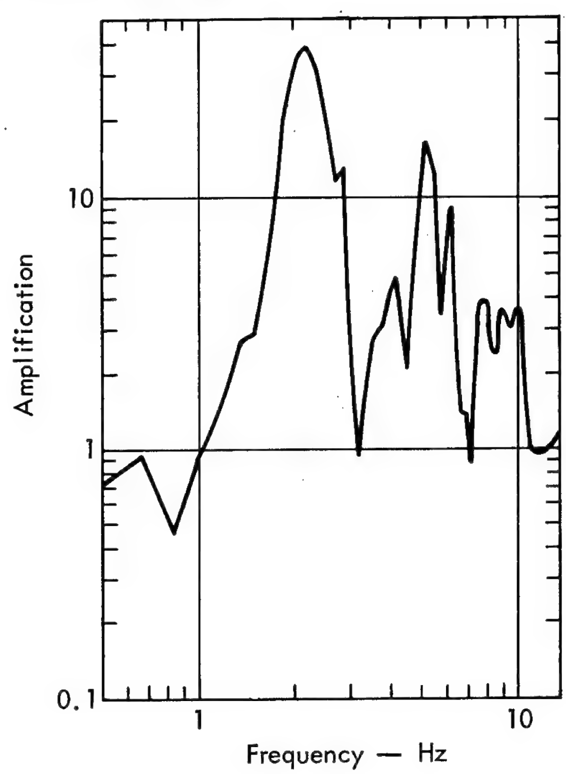

Fig. 14. Ratio of PSD's for Station 1 over Station 3 (z component).

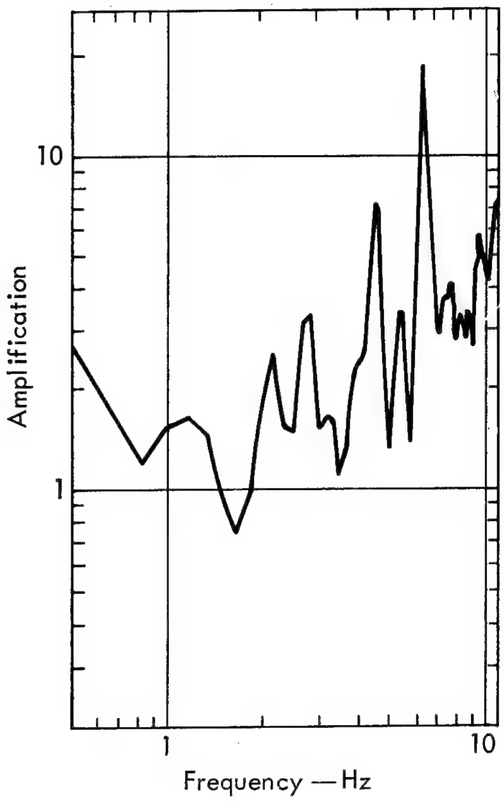

Fig. 15. Ratio of PDS's for Station 2 over Station 3 (x component).

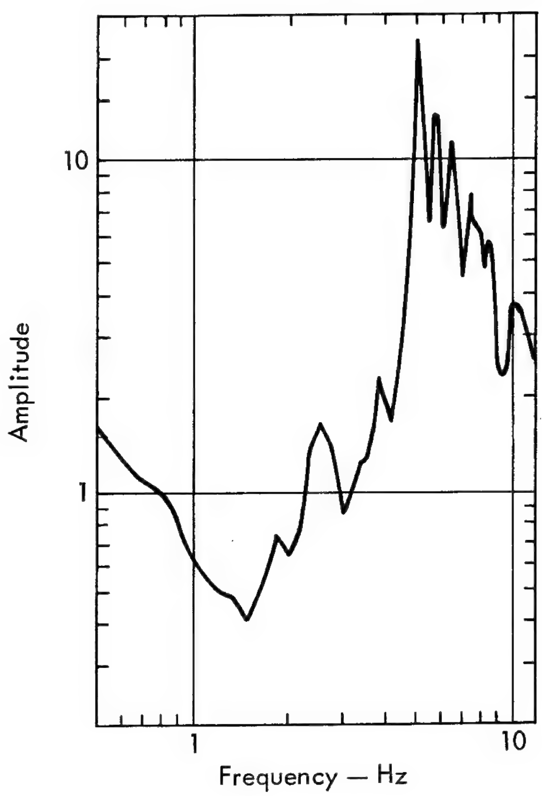

Fig. 16. Ratio of PSD's for Station 2 over Station 3 (y component).

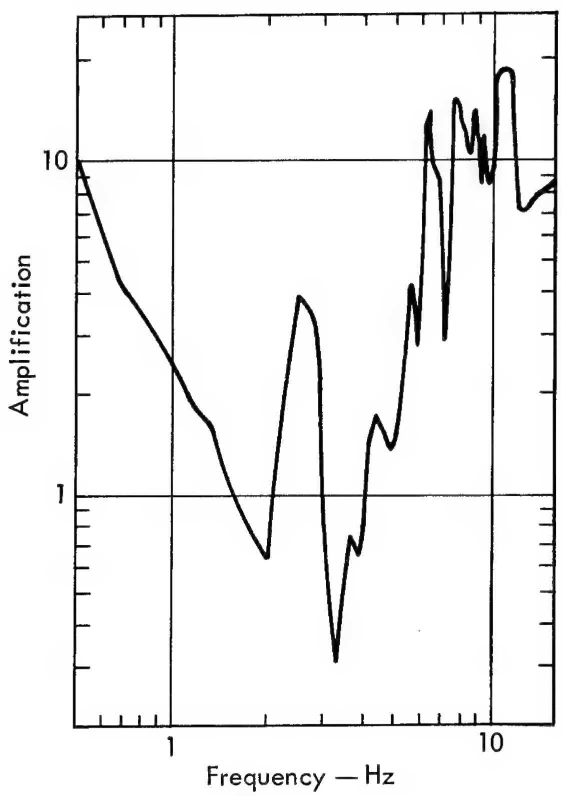

Fig. 17. Ratio of PSD's for Station 2 over Station 3 (z component).

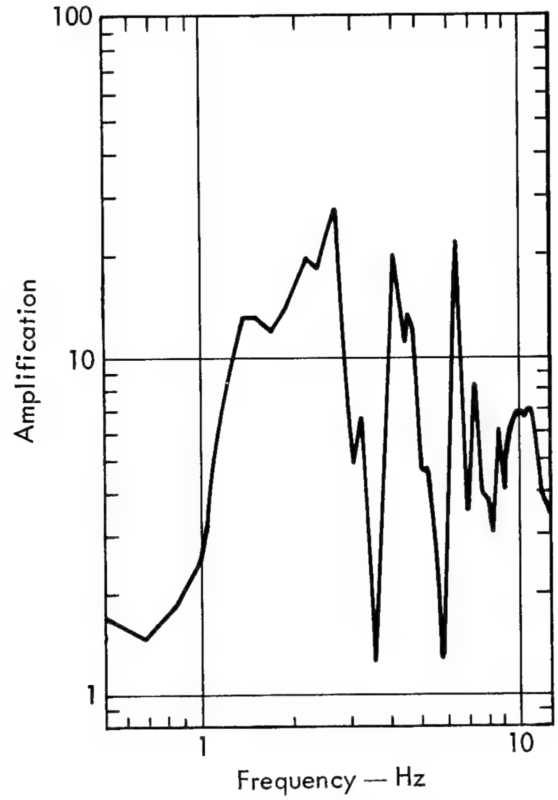

Fig. 18. Ratio of PSD's for Station 4 over Station 3 (x component).

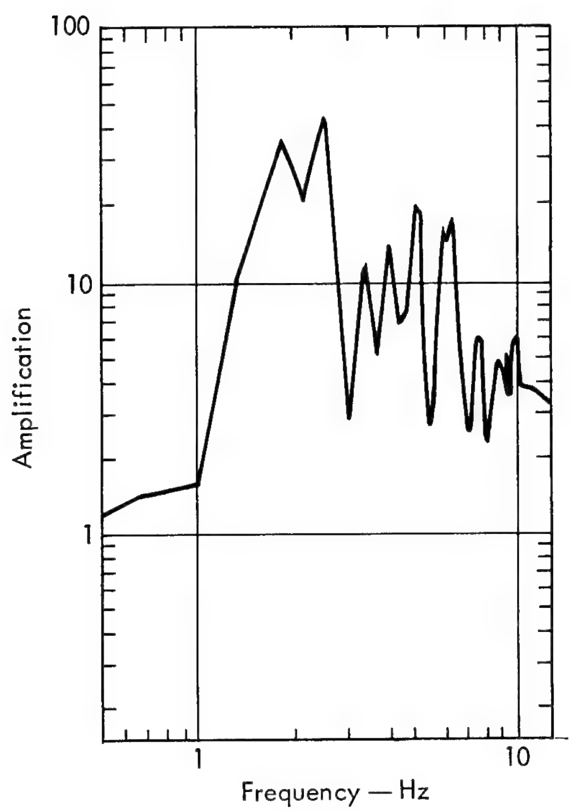

Fig. 19. Ratio of PSD's for Station 4 over Station 3 (y component).

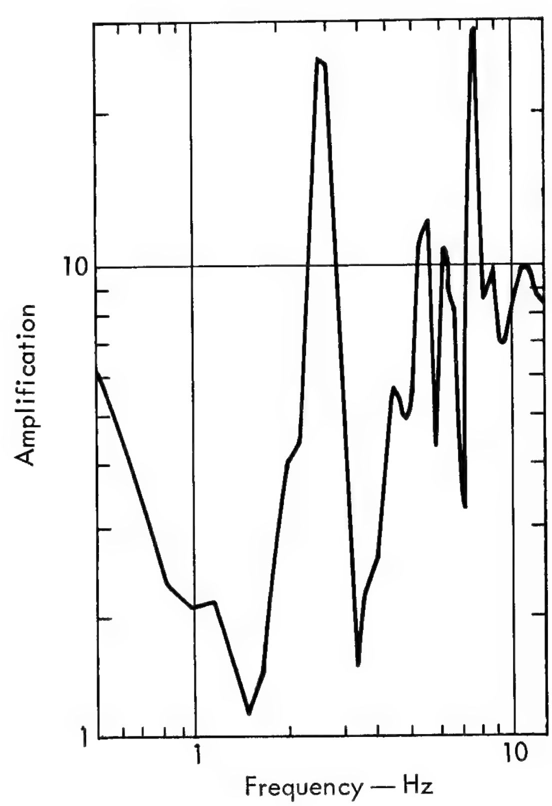

Fig. 20. Ratio of PSD's for Station 4 over Station 3 (z component).

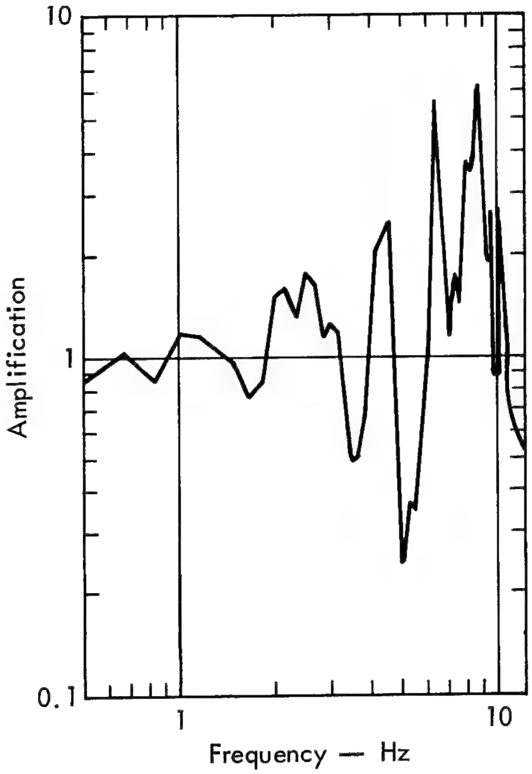

Fig. 21. Ratio of PSD's for Station 5 over Station 3 (x component).

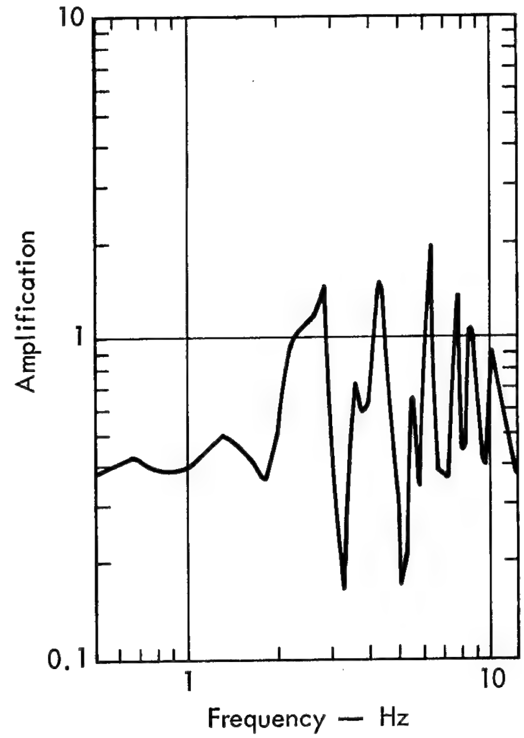

Fig. 23. Ratio of PSD's for Station 5 over Station 3 (z component).

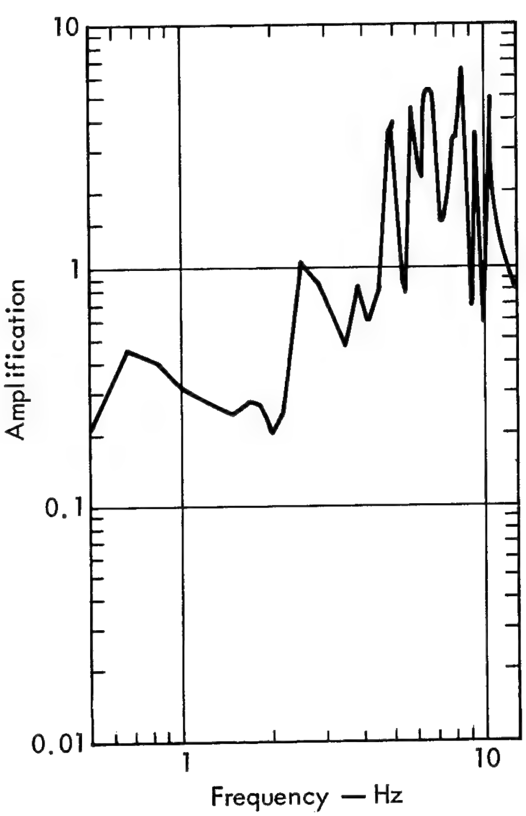

Fig. 22. Ratio of PSD's for Station 5 over Station 3 (y component).

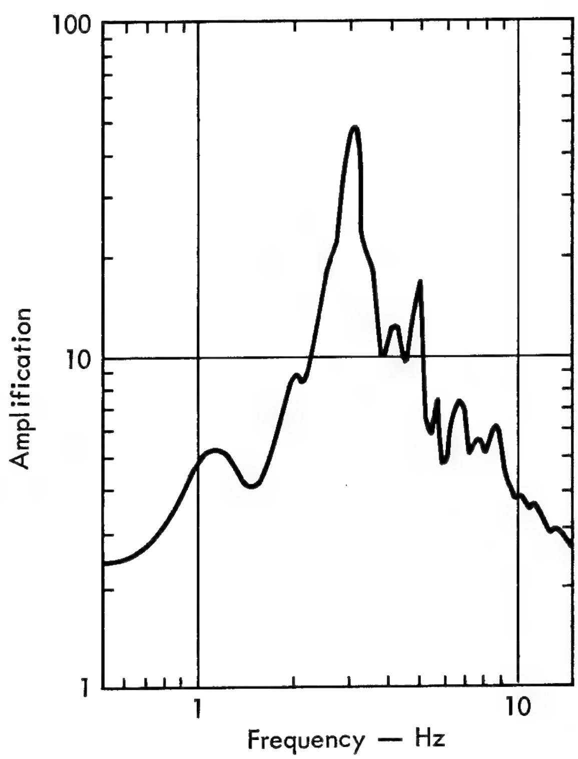

Fig. 24. Ratio of PSD's for Station 6 over Station 7 (x component).

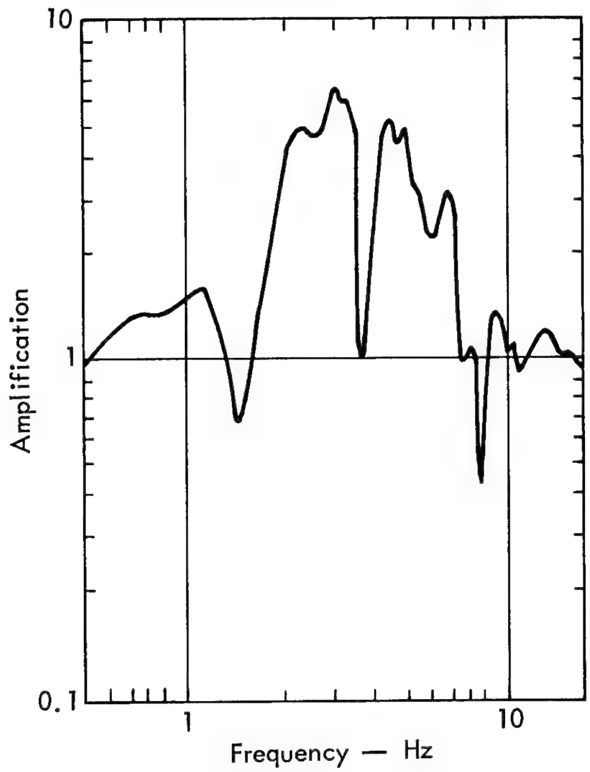

Fig. 25. Ratio of PSD's for Station 6 over Station 7 (y component).

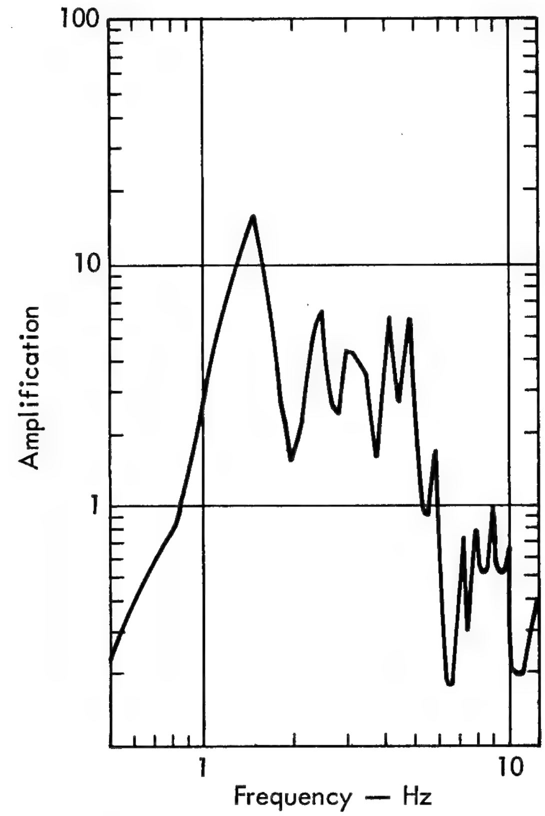

Fig. 27. Ratio of PSD's for Station 1 over Station 2 (x component)

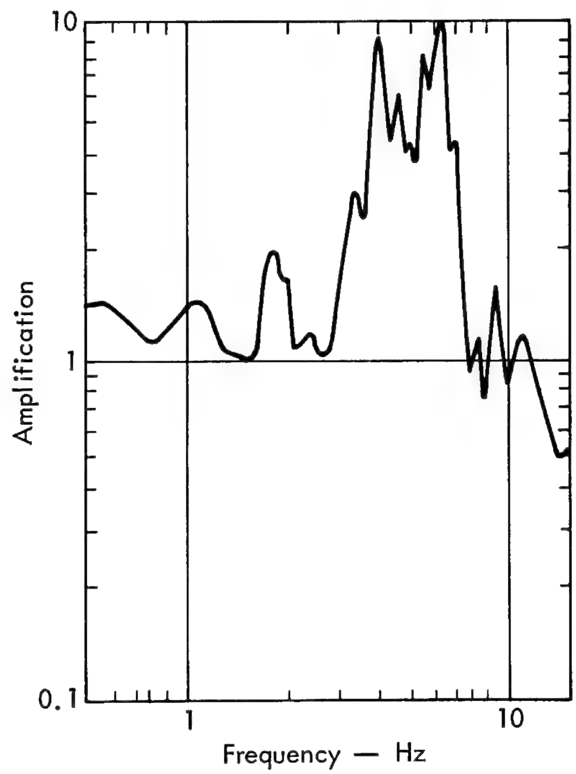

Fig. 26. Ratio of PSD's for Station 6 over Station 7 (z component).

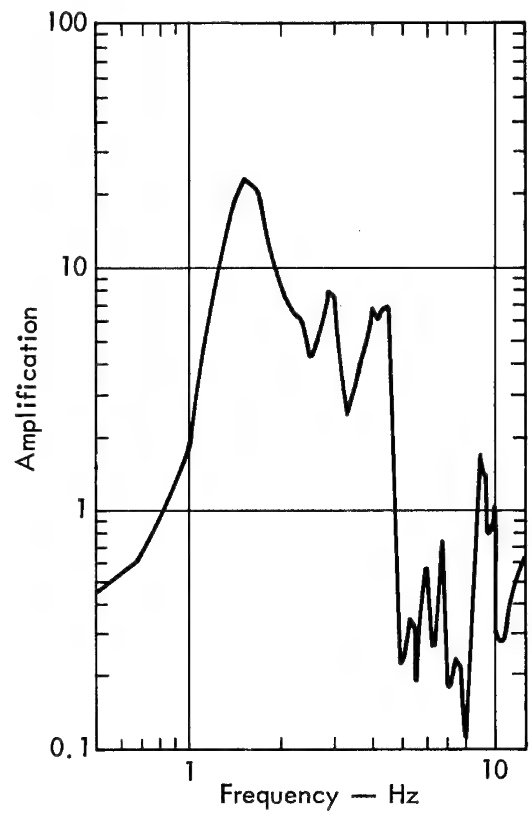

Fig. 28. Ratio of PSD's for Station 1 over Station 2 (y component).

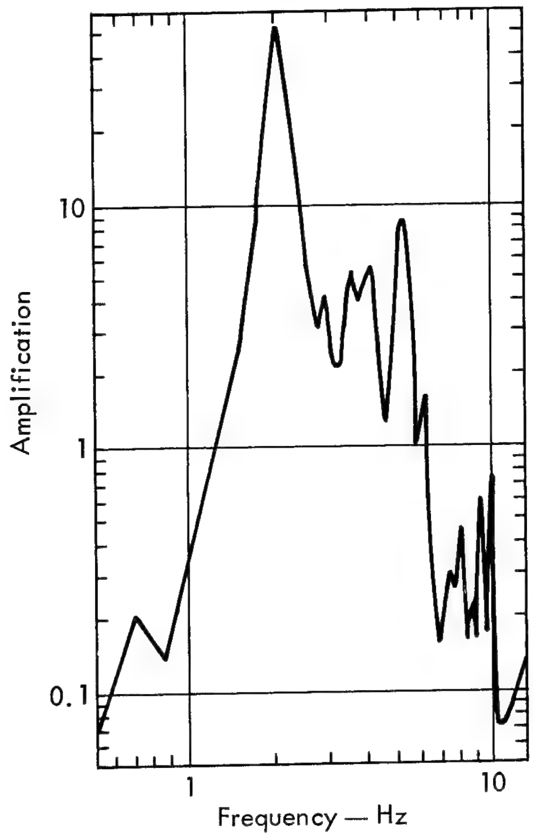

Fig. 29. Ratio of PSD's for Station 1 over Station 2 (z component).

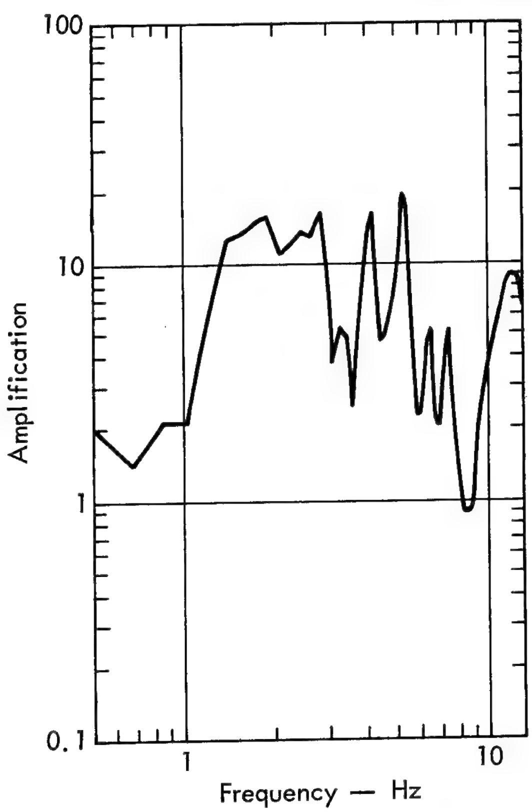

Fig. 30. Ratio of PSD's for Station 4 over Station 5 (x component).

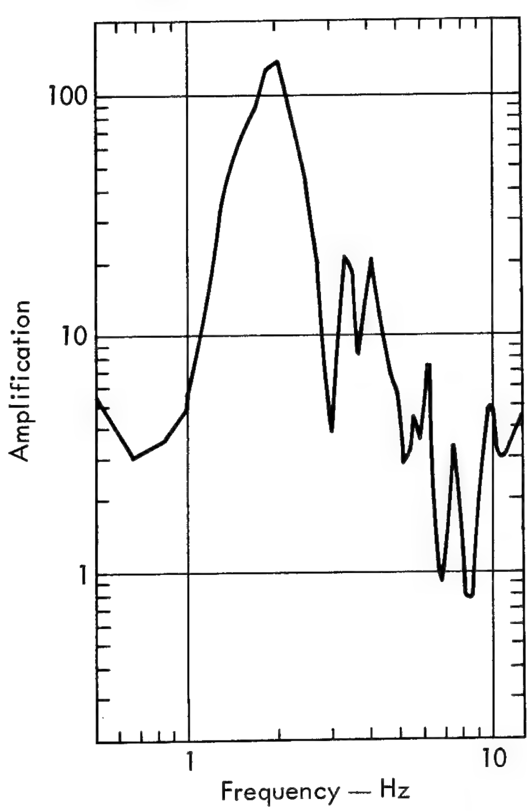

Fig. 31. Ratio of PSD's for Station 4 over Station 5 (y component).

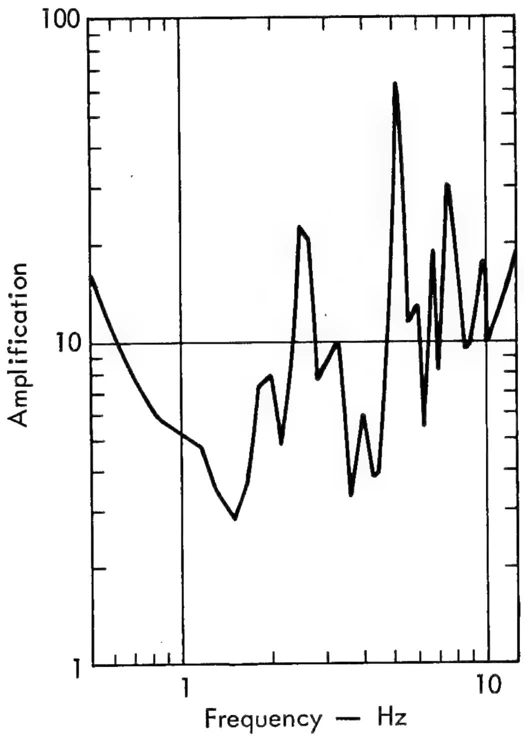

Fig. 32. Ratio of PSD's for Station 4 over Station 5 (z component).

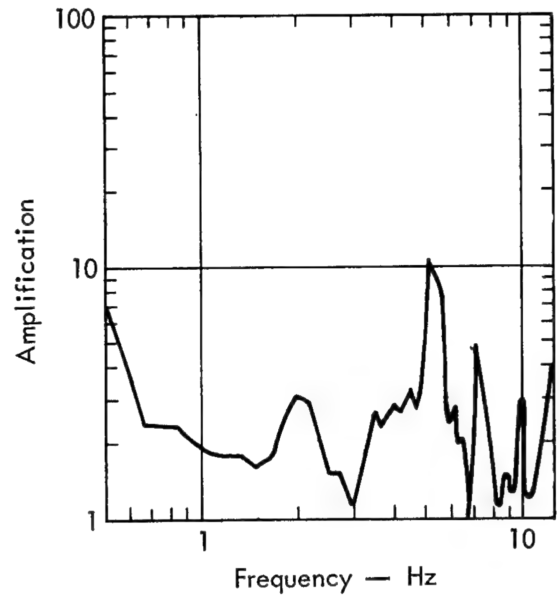

Fig. 34. Ratio of PSD's for Station 2 over Station 5 (y component).

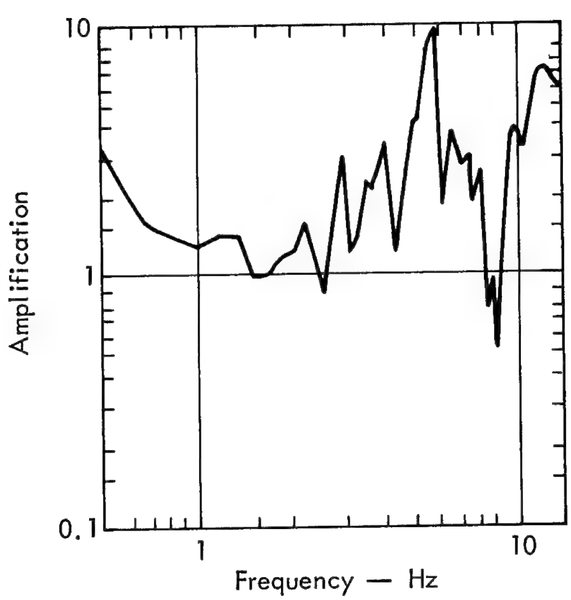

Fig. 33. Ratio of PSD's for Station 2 over Station 5 (x component).

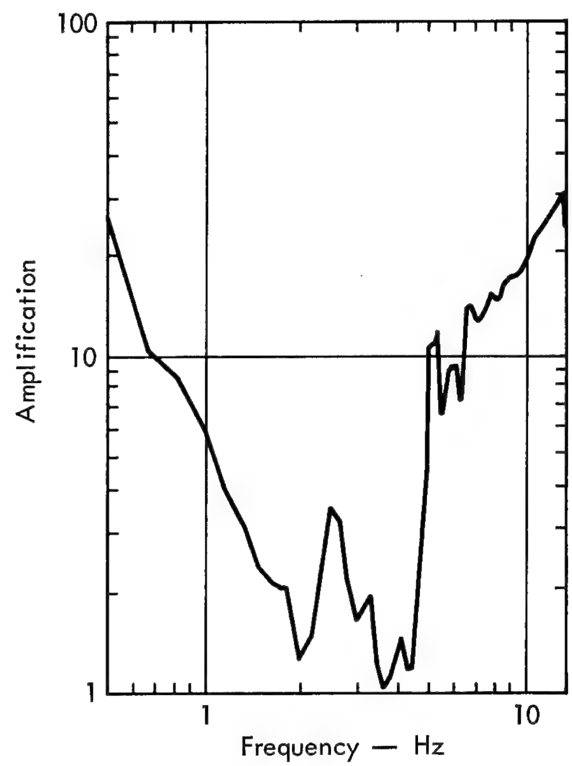

Fig. 35. Ratio of PSD's for Station 2 over Station 5 (z component).

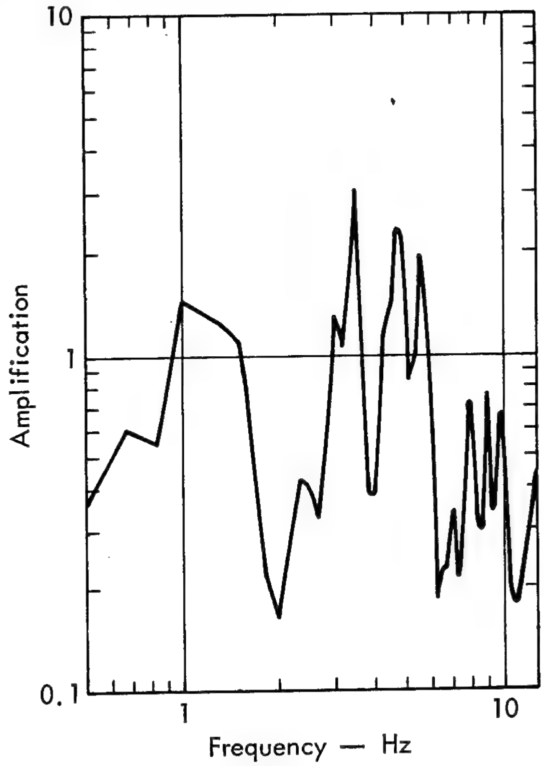

Fig. 36. Ratio of PSD's for Station 1 over Station 4 (x component).

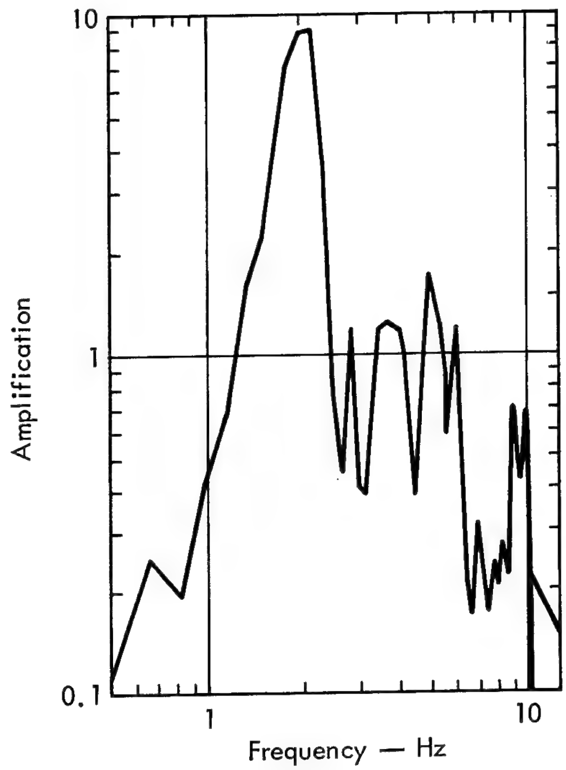

Fig. 38. Ratio of PSD's for Station 1 over Station 4 (z component).

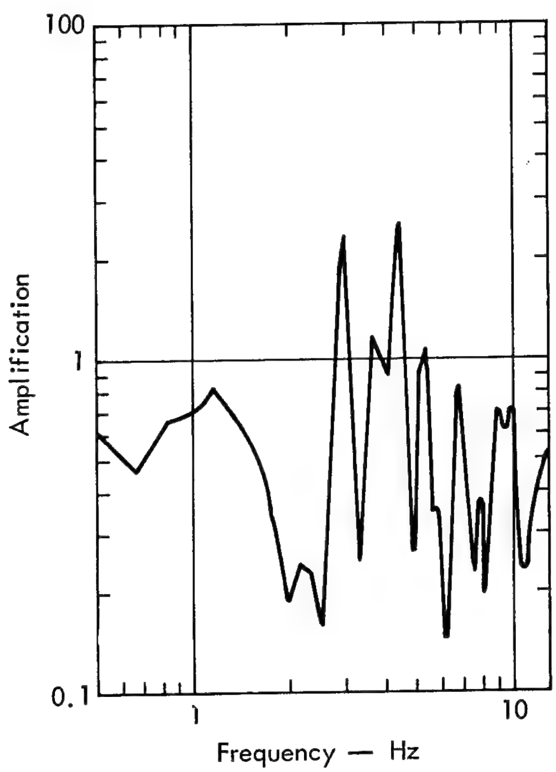

Fig. 37. Ratio of PSD's for Station 1 over Station 4 (y component).

above 5 Hz. Station 2 is known to have about 50 ft of fill on top of bedrock. Assuming a half wave length of 50 ft and a resonant frequency of 5 Hz, the shear wave velocity in the fill is 500 ft/sec, a low but not unreasonable value for the toe material.

A very crude calculation for the entire dam is to assume that the section through Station 1 is a simple column 400 ft in height which is unaffected in its x motion by the constraints at the abutments. A half wave length of 400 ft and a resonance of 1.4 Hz (see Fig. 12) result in a shear wave velocity of 1120 ft/sec. This value agrees very well with the 1270 ft/sec that Keightley measured in the Bouquet Canyon earth fill dam.[6]

The El Vado Dam, with its steel membrane becomes difficult to analyze. One

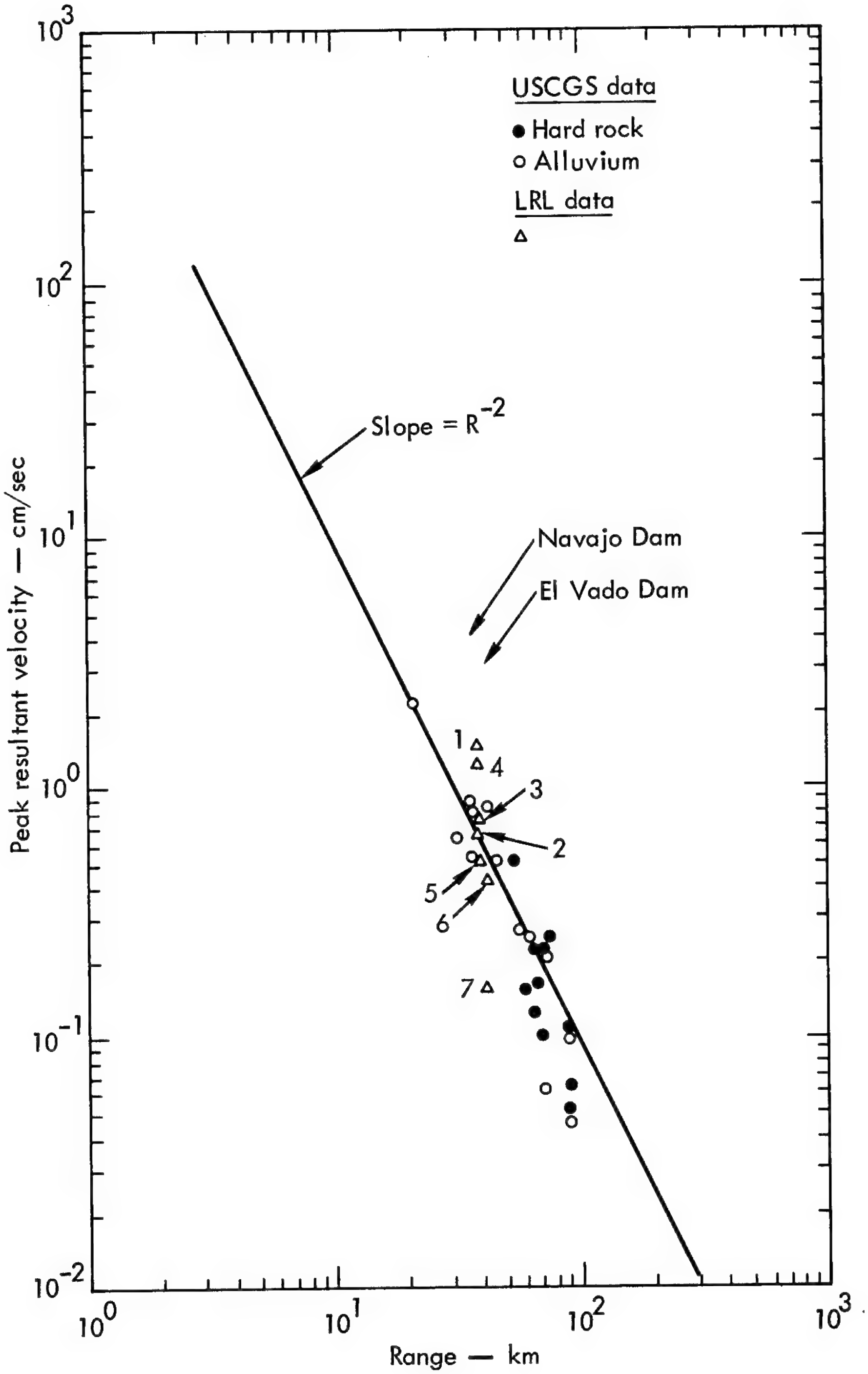

Fig. 39. Peak resultant velocities on Navajo and El Vado Dams compared with standard USC&GS ground motion stations (line is not fitted to data but is shown for comparison purposes).

might expect a higher average shear wave velocity as a result of the steel. However the half wave length of 180 ft and a resonant frequency of 3 Hz in the x mode (see Fig. 24) indicate a shear wave velocity of 1080 ft/sec. Apparently the mass of the steel is not sufficient to drive the bulk of the earth fill, and the steel can effectively be ignored in the analysis. The y mode (see Fig. 25) shows two broad peaks in the amplification at 3.0 and 4.5 Hz and the z mode (see Fig. 26) has strong peaks at 3.6 and 6.0 Hz and a small peak at 1.7 Hz.

The amplifications of the PSD shown in Figs. 12 through 26 are frequency-dependent and are therefore much different from the values of F_2 and F_3 in Table II which ignore frequency. For some frequencies the PSD amplification is as high as 40 or 50 (Figs. 24 and 14). This would indicate an increase in velocity of 6 or 7 times base motion in some frequencies. However, most of the PSD's on the crest are about 5 to 10 times the base motion. This indicates an average velocity amplitude ratio of 2 to 3 which is in agreement with Table I.

Conclusions and Recommendations

1. The maximum motions on the dam crest did not occur at the same frequencies as the maximum amplification factors. This is primarily because much of the motion in the base signal was not at the resonant frequencies of the dams. Considerably greater response motion might have been noted had the incoming signal contained more significant motions at frequencies of 1.5 and 2.5 Hz. The motions on the dams were not significantly greater than what might have been expected in natural alluvial geology.
2. The level of motions experienced on the dam in this study are very small and certainly well below any failure level. It is not certain how far up in motion one can feel safe in applying the results of this study to other cases. Clearly one needs more data at larger motions to find out what changes in response occur as one approaches the nonlinear response range.
3. Power spectral density is a valuable tool in describing ground motion and structures response. The results are entirely consistent with other techniques, and information is gained which is not available through other common methods.
4. One deficiency of the PSD is the loss of phase information and the resulting loss of internal stress and strain data. To gain this type of data a more sophisticated instrument system must be used in which all stations are correlated in real time. It is hoped that theoretical analysis techniques will soon be easily available to give a comparison to this type of measurements program.

Acknowledgments

The author wishes to express his thanks to John Lane and Kenneth Olsen of the Lawrence Radiation Laboratory for their extended efforts in the field in support of this study, and to the Bureau of Reclamation personnel in the Durango office and at the Navajo and El Vado Dams for their cooperation and assistance.

References

1. Bureau of Reclamation, Navajo Dam and Reservoir; Technical Record of Design and Construction, Denver, Colorado, November 1966.
2. Letter from Secretary of Interior, San Juan-Chama and Navajo Indian Projects, 86th Congress 2nd Session, House Document No. 424, U. S. Government Printing Office, Washington, June 20, 1960.
3. D. V. Power, Intermediate Range Ground Motions for Pre-Gondola II and Associated Events, Lawrence Radiation Laboratory, Livermore, Rept. UCRL-50433, April 1968 (also published as PNE-1115).
4. R. B. Blackman, and J. W. Tukey, The Measurement of Power Spectra from the Point of View of Communications Engineering (Dover Publications, New York, N. Y., 1959).
5. Environmental Research Corporation, Observed Ground Motion Data Project Gasbuggy, Interim Report, Nevada Operations Office, Las Vegas, Rept. NVO-1163-144, May 1968.
6. W. O. Keightley, A Dynamic Investigation of Bouquet Canyon Dam, Earthquake Engineering Research Laboratory, California, September 1964.

Distribution

LRL Internal Distribution

Michael M. May/D. Sewell
R. E. Batzel
H. L. Reynolds
J. W. Gofman
R. Herbst
A. C. Haussmann
C. A. McDonald
J. W. Rosengren
E. Teller
C. M. Van Atta
G. C. Werth
J. E. Carothers
G. D. Dorough
F. S. Eby
E. H. Fleming
W. B. Harford
G. H. Higgins
F. Holzer
J. T. Cherry
J. S. Kahn
J. S. Kane
J. B. Knox
B. C. Hughes
T. Perlman
P. H. Moulthrop
M. D. Nordyke
B. Rubin
D. Dorn
P. C. Stevenson
H. A. Tewes
C. E. Williams/P. E. Coyle
W. Woodruff
D. Lombard
J. Korver
D. Rawson
R. Heckman
C. Smith
M. Nadolski
T. Barlow
S. Warner
J. Lane
K. Olsen
R. Rossman
L. Crooks/E. Harpe, Mercury
TID Berkeley
TID File 30

External Distribution

S. Smith
H. Gevertz
L. Truby
R. Lemon
P. Randolph
M. Spitler
J. Arnett
D. Power 25
L. Rogers
El Paso Natural Gas Company
El Paso, Texas

W. Martin
H. Kendrick
W. Cutler
W. Musick
El Paso Natural Gas Company
Farmington, New Mexico

W. Watkins
R. Swenarton
U. S. Bureau of Mines
Washington, D. C.

C. Atkinson
D. Ward
U. S. Bureau of Mines
Bartlesville, Oklahoma

S. West
U.S. Geological Survey
Denver, Colorado

W. Hale
U.S. Geological Survey
Albuquerque, New Mexico

J. Kelly 5
C. Gerber
R. Hamburger
W. Oakley
U.S. Atomic Energy Commission
Division of Peaceful Nuclear Explosives
Washington, D. C.

A. Garner
U. S. Atomic Energy Commission
Division of Military Applications
Washington, D. C.

J. Philip
E. Campbell
R. Southwick
U.S. Atomic Energy Commission
San Francisco Operations Office
Berkeley, California

External Distribution (Continued)

J. Reeves
R. Miller
R. Thalgott
D. Edwards
R. Kinnaman
R. Loux
H. Vermillion
U.S. Atomic Energy Commission
Nevada Operations Office
Las Vegas, Nevada

R. F. Beers
Environmental Research Corporation
Alexandria, Virginia

W. Perret
B. Murphey
Sandia Corporation
Albuquerque, New Mexico

L. Aamodt
R. Campbell
Los Alamos Scientific Laboratory
Los Alamos, New Mexico

J. L. Merritt
TRW Systems
San Bernardino, California

J. O. Putnam
Space and Missile Systems Organization
Norton Air Force Base, California

R. W. Henny
Air Force Weapons Laboratory
Kirtland Air Force Base
Albuquerque, New Mexico

TID-4500, UC-35, Nuclear Explosions—Peaceful Applications 255

Printed in USA. Available from the Clearinghouse for Federal Scientific and Technical Information, National Bureau of Standards, U.S. Department of Commerce, Springfield, Virginia 22151
Price: Printed Copy $3.00; Microfiche $0.65.

WF/rt